



Analysis of Stress State and Damage Characteristics of the Cement Sheath

Feng Xu^{1,2*}, Qingyang Ren^{2*}, Hao Ling^{3*}, Hongwu Yin⁴, Xiaogui Zhou⁵, Zhongshuai Liu¹ and Guangqing Yang¹

¹China Merchants Chongqing Communications Research & Design Institute Co., Ltd., Chongqing, China, ²School of Civil Engineering, Chongqing Jiaotong University, Chongqing, China, ³Chongqing Vocational College of Culture and Arts, Chongqing, China, ⁴Guangzhou Expressway Co., Ltd., Guangzhou, China, ⁵Department of Civil and Environmental Engineering, Rensselaer Polytechnic Institute, Troy, NY, United States

OPEN ACCESS

Edited by:

Guowen Xu,
Colorado School of Mines,
United States

Reviewed by:

Hongyu Gu,
Chengdu Geological Survey Center,
China
Hu Guo,
China University of Petroleum, Beijing,
China
Mingjing Lu,
SINOPEC, China

*Correspondence:

Feng Xu
scxufeng@163.com
Qingyang Ren
qyren@cqjtu.edu.cn
Hao Ling
276486871@qq.com

Specialty section:

This article was submitted to
Carbon Capture, Utilization and
Storage,
a section of the journal
Frontiers in Energy Research

Received: 11 December 2021

Accepted: 21 February 2022

Published: 08 April 2022

Citation:

Xu F, Ren Q, Ling H, Yin H, Zhou X,
Liu Z and Yang G (2022) Analysis of
Stress State and Damage
Characteristics of the Cement Sheath.
Front. Energy Res. 10:833388.
doi: 10.3389/fenrg.2022.833388

The sealing problem of the cement sheath often appears in gas wells for underground energy exploitation, especially when horizontal multistage fracturing technology is used in the shale gas industry. In this article, according to the elastic–plastic mechanics and Mohr–Coulomb yield criteria, an analytical solution of the equations is obtained by considering the effect of pressure on the fluid column, volume shrinkage, or expansion and geological characteristics on the initial stress of the cement sheath. The analysis of the example indicates that the smaller the initial stress of the cement sheath, the lower its radial stress and circumferential stress, which is under the maximum inner casing pressure of 150 MPa. With the increase of initial stress of the cement sheath, it is easier for the first and second interfaces to enter the plastic and damage state for the cement sheath. The smaller the initial stress of the cement sheath, the earlier the damage appears, and it develops with the increase of inner casing pressure more quickly. When the initial stress of the cement sheath is less than 7.9 MPa, the damage factor finally reaches 1 with the increase of internal casing pressure; however, when the initial stress of the cement sheath is greater than 34.2 MPa, the damage factor always remains 0 with the increase of inner casing pressure. The results preliminarily revealed that the initial stress of the cement sheath plays a decisive role in promoting its integrity and may provide guidance for the choice of the formula of cement and construction methods in the oil field.

Keywords: cement sheath integrity, initial stress, Mohr–Coulomb yield criteria, theoretical solution, damage factor, shale gas

1 INTRODUCTION

Energy is the cornerstone of human survival and human social development. Global unconventional oil and gas resources account for 80% of oil and gas resources and will become the main energy in the future (Xu et al., 2022). Cement slurry cementing is widely used in underground energy exploitation. Due to the influence of cement characteristics, formation pressure, temperature, and post-fracturing construction operations, the seal integrity of the cement sheath meets a serious challenge, which causes the plastic ring of the cement sheath yield; the first and second interface micro-seam joints and the annulus pressure are extremely prominent (Wang et al., 2013).

In the process of multistage fracturing of horizontal wells, the cement sheath is constantly affected by the cyclic alternation of low temperature (fracturing fluid) and high temperature (formation), which could cause shear, tensile, and interface separation damage easily, resulting in shale gas entering into the cement sheath fracture and generating annular pressure problems (Saint-Marc,

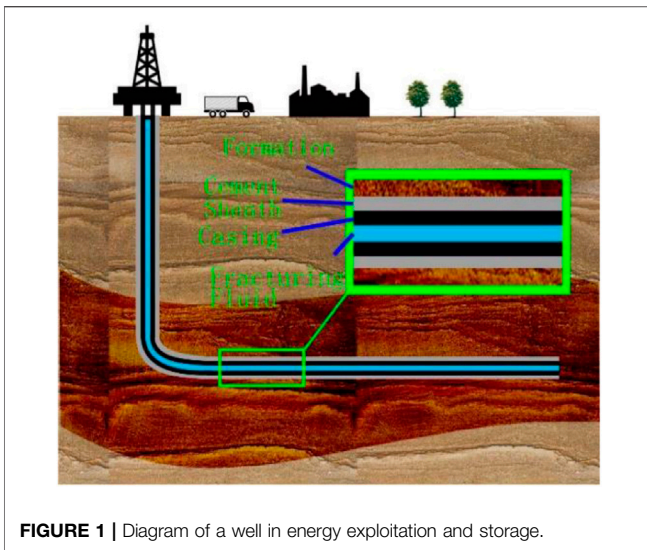


FIGURE 1 | Diagram of a well in energy exploitation and storage.

2008), as shown in **Figures 1, 2**. The first or second interface separation indicates bond failure at the inner/outer boundary of the cement sheaths for the plastic deformation of the cement sheath cannot be restored to the initial state under circulating pressure in casing, which results in discontinuous displacement of casing–cement sheath-formation. The shear damage indicates the shear stress of the cement sheath that exceeds the friction stress in the Mohr–Coulomb criterion. The tensile failure indicates that the tensile stress exceeds tensile strength. Therefore, it is essential to investigate the stress distribution of the casing–cement sheath-formation system during construction in cementing operations.

Domestic and foreign scholars have performed a lot of research on the integrity of cement sheath seals (Liu et al., 2020; Chen et al., 2021). Zhang et al. (2017) studied the sealing characteristics of the cement sheath in the fracturing process by simulation experiments and found that with the increase of the number of fracturing alternating stress, the plasticity deformation continues to accumulate and eventually produces microcracks; Fang et al. (1995) and Yin et al. (2006) gave the elastic analytical solution of casing–cement

sheath-formation under nonuniform ground stress under ideal conditions; Li et al. (2005a) analyzed the elastoplastic theory of casing, cement sheath, and shaft wall rock and gave the elastoplastic analytical solution. Deng et al. (1994) deduced the formula for calculating the stress state of the casing and cement sheath under the creep load of various nonuniform surrounding rocks; Jing et al. (2009) deduced the theoretical calculation formulas of thermal stress and thermal displacement of the casing–cement sheath-formation coupling system based on the theory of elastic mechanics and thermodynamics and analyzed the system heat, the radial distribution of stress, and thermal displacement; Xu et al. (2015) coupled the thermal stress and elastoplastic mechanics to give the analytical solution and numerical solution of the stress and deformation of the casing–cement sheath-formation system; Li et al. (2010) calculated the stress of the cement sheath and its deformation characteristics under high temperature and nonuniform stress conditions. Li et al. (2005b) carried out a theoretical calculation method to investigate the influence of the cement sheath elastic modulus on the stress state of the composite; Zhang et al. (2013) studied the impact of the elastic parameters of the cement sheath on the structural integrity of casing–cement sheath-formation by ANSYS software.

However, all of the aforementioned studies have applied the far-field stress directly to the casing–cement sheath-formation combination, neglecting the stress release of the wellbore after drilling and the entire process of stress application. Based on this, to study the mechanical characteristics of the whole process of cement solidification, the author defines the stress state of the cement sheath formed by solidification of the cement slurry in this article as the initial stress of the cement sheath, and at this moment, it receives equal radial and circumferential stress at each point. The cementing cement sheath-forming process includes the stress release of the wellbore after drilling, the cement slurry pressure causes the wellbore and the casing to deform coordinately, and the cement slurry solidification shrinkage or expansion, and the initial stress of the cement sheath is subjected to the liquid column pressure during the solidification process, volume shrinkage or expansion,

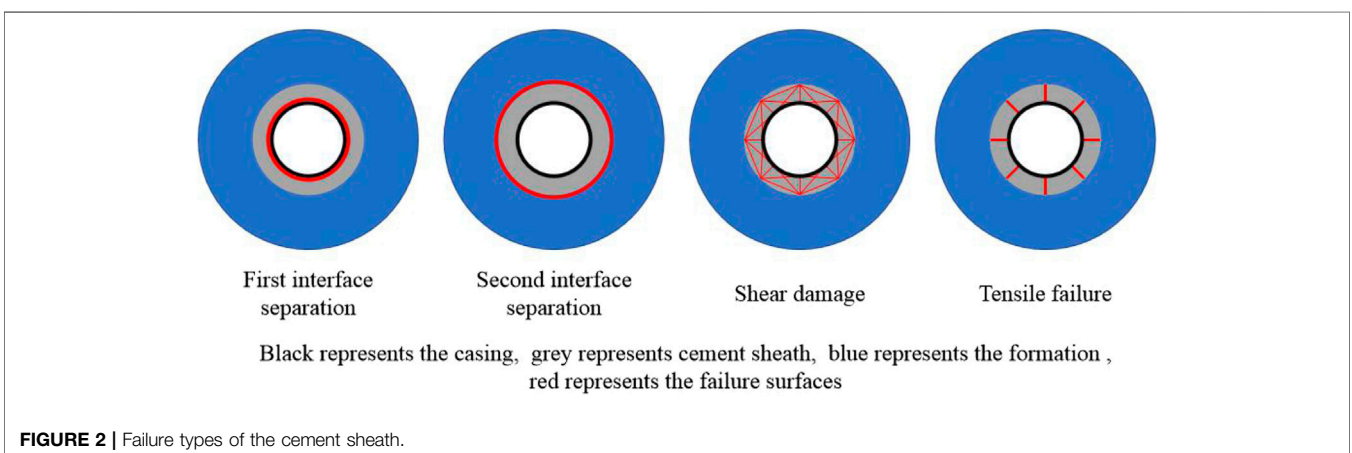


FIGURE 2 | Failure types of the cement sheath.

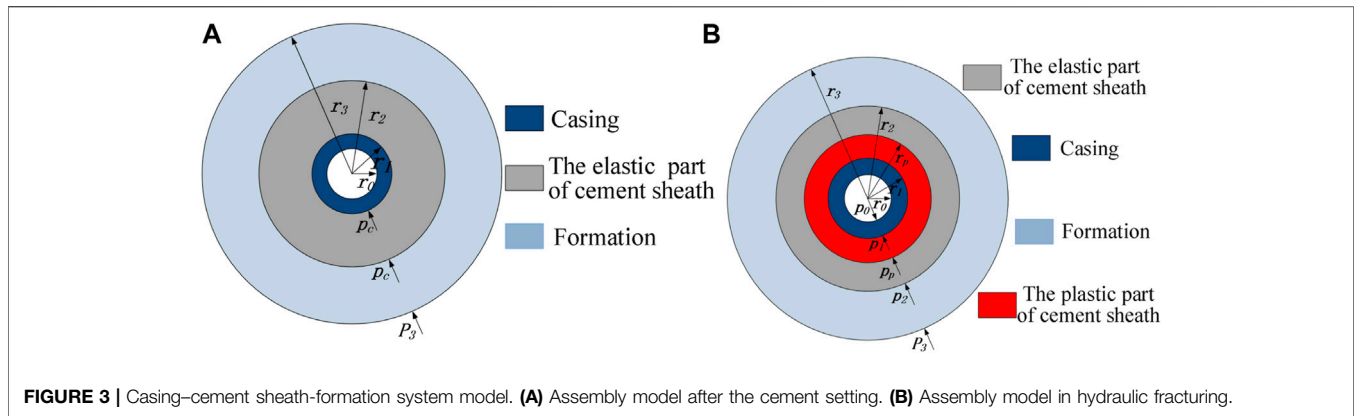


FIGURE 3 | Casing–cement sheath–formation system model. **(A)** Assembly model after the cement setting. **(B)** Assembly model in hydraulic fracturing.

formation characteristics, and other factors. In order to investigate the influence of different initial stresses on the mechanical characteristics of the casing–cement sheath–formation system after solidification of cement slurry, the mechanical model of the casing–cement sheath–formation system considering the initial stress state of the cement sheath is established by using the elastoplastic theory.

2 CASING–CEMENT SHEATH-FORMATION SYSTEM MODEL

The cement sheath often exceeds hundreds of meters in the axial direction, and it is restricted deformation in the axial direction. The model of casing–cement sheath–formation can be simplified to the plane strain model. Before conducting research, the following assumptions need to be made on the model:

- (1) During the study, it is assumed that the casing and formation are elastic materials because the formation stress does not exceed the yield stress of the casing and rock (Xu et al., 2017).
- (2) During the study, it is assumed that the cement sheath is an ideal elastic–plastic material and meets the Mohr–Coulomb criterion (Xu et al., 2021).
- (3) The initial stress formed by cement solidification is equal everywhere, that is, the first and second interface contact stresses are equal, and the specific parameters are shown in **Figure 3**;
- (4) The casing is completely centered, that is, the casing and the cement sheath are concentric rings, and the cement is completely filled; this article adopts the elastic mechanical symbol convention, positive tensile stress, and negative compressive stress.

Figure 3A shows the physical size and stress state of the casing–cement sheath–formation system model after solidification and coordinated deformation of cement. **Figure 3B** shows the physical model and mechanical parameters of the composite during fracturing, that is, the physical model of **Figure 3B** is due to **Figure 3A**. The physical

model is caused by the application of internal pressure in the casing. In the figure, r_0 , r_1 , r_2 , r_3 , and r_p , respectively, represent the inner and outer diameters of the casing of the composite model after cement solidification, the outer diameter of the cement sheath, the outer boundary of the surrounding rock, and the elastic–plastic interface of the cement sheath; p_c indicates the initial cement sheath after solidification of the cement. The stresses, p_0 , p_1 , p_2 , p_p , and p_3 , respectively, indicate the pressure in the casing of the composite during the fracturing process, the first interface contact stress, the second interface contact stress, the elastoplastic interface stress of the cement sheath, and the far-field stress of the formation.

2.1 Establishment of a Combination Mechanics Models

For cement sheaths with planar problems, the failure criterion is generally based on the Mohr–Coulomb yield criterion. Because the first and second interfacial stresses are equal after the cement stone solidifies, the calculated cement sheath satisfies $\sigma_\theta = \sigma_r = -p_c$ everywhere. As the internal pressure of the casing increases, $\sigma_\theta > -p_c > \sigma_r$ always holds. Then, the Mohr–Coulomb yield criterion is as follows:

$$\frac{1}{2}(\sigma_\theta - \sigma_r) + \frac{1}{2}(\sigma_\theta + \sigma_r)\sin\varphi - C\cos\varphi = 0. \tag{1}$$

As shown in **Figure 3**, when the pressure p_0 in the casing is increased to a certain extent, a plastic zone appears inside the initially elastic cement sheath, and as the internal pressure increases, the shaping zone gradually expands outward. The stress component of the plastic zone of the cement sheath should satisfy the equilibrium equation, namely,

$$\frac{d\sigma_r}{dr} + \frac{\sigma_r - \sigma_\theta}{r} = 0. \tag{2}$$

When **Eqs 1, 2** are jointly solved and the boundary condition $r = r_1$, $\sigma_r = -p_1$ is taken into the aforementioned equation, and the expression of the stress component of the plastic zone of the cement sheath ($r_1 \leq r \leq r_p$) can be obtained as follows (Zhaowei and Yongen, 2009):

$$\begin{cases} \sigma_r = C \cot \varphi \left[1 - \left(1 + \frac{p_1}{C \cot \varphi} \right) \left(\frac{r}{r_1} \right)^{B-1} \right] \\ \sigma_\theta = C \cot \varphi \left[1 - B \left(1 + \frac{p_1}{C \cot \varphi} \right) \left(\frac{r}{r_1} \right)^{B-1} \right] \end{cases}, \quad (3)$$

where $B = (1 - \sin \varphi) / (1 + \sin \varphi)$, C is the cement sheath cohesion, and φ is the cement sheath internal friction angle.

When the cement sheath $r = r_p$, $\sigma_r = -p_p$ is substituted into the formula (Eq. 3), and the stress expression at the elastic-plastic interface of the cement sheath is obtained as follows:

$$p_p = C \cot \varphi \left[\left(1 + \frac{p_1}{C \cot \varphi} \right) \left(\frac{r_p}{r_1} \right)^{B-1} - 1 \right]. \quad (4)$$

The stress component of the elastic zone of the cement sheath ($r_p \leq r \leq r_2$) is:

$$\begin{cases} \sigma_r = \frac{r_p^2 r_2^2 (p_2 - p_p)}{r_2^2 - r_p^2} \frac{1}{r^2} + \frac{r_p^2 p_p - r_2^2 p_2}{r_2^2 - r_p^2} \\ \sigma_\theta = -\frac{r_p^2 r_2^2 (p_2 - p_p)}{r_2^2 - r_p^2} \frac{1}{r^2} + \frac{r_p^2 p_p - r_2^2 p_2}{r_2^2 - r_p^2} \end{cases}. \quad (5)$$

When the elastic zone $r = r_p$, it is just in the plastic critical state and meets the Mohr-Coulomb failure criterion. Substituting the values of σ_r and σ_θ obtained by substituting the elastic region $r = r_p$ into Eq. 5 into Eq. 1, we obtain the following equation:

$$\frac{r_2^2 (p_2 - p_p)}{r_2^2 - r_p^2} - \frac{r_p^2 p_p - r_2^2 p_2}{r_2^2 - r_p^2} \sin \varphi + C \cos \varphi = 0. \quad (6)$$

2.2 Establishment of Assembly Displacement Relationship

The casing-cement sheath-formation system has continuity at the first and second interface displacements, since the stress state in Figure 3 is formed by the stress state of the (1) stress state and the internal pressure of the casing during the fracturing stage, and the casing is formed. The change in the displacement of the cement sheath-formation system is due to the application of the internal pressure of the casing, so the displacement should be the displacement change caused by the internal pressure of the casing. The actual displacement generated by the elastic zone fracturing process shall be the change of the displacement of the composite during the fracturing process subtracted by the displacement change of the composite during the solidification process of the cement stone:

$$u|_{r=r_i} = u|_{r=r_i}^1 - u|_{r=r_i}^0. \quad (7)$$

According to the Lamé formula (Jin and Chen, 2012), the radial displacement expressions of the casing, cement sheath, and borehole elastic region are as follows:

The displacement of the outer wall for the casing is:

$$\begin{cases} u_{ca}|_{r=r_1}^1 = \frac{(1 + \mu_1)r_1}{E_1(r_1^2 - r_0^2)} [r_0^2(p_0 - p_1) + (1 - 2\mu_1)(r_0^2 p_0 - r_1^2 p_1)] \\ u_{ca}|_{r=r_1}^0 = \frac{(1 + \mu_1)r_1}{E_1(r_1^2 - r_0^2)} [r_0^2(-p_c) + (1 - 2\mu_1)(-r_1^2 p_c)] \end{cases}. \quad (8)$$

The displacement of borehole wall is:

$$\begin{cases} u_f|_{r=r_2}^1 = \frac{(1 + \mu_3)r_2}{E_3(r_3^2 - r_2^2)} [r_3^2(p_2 - p_3) + (1 - 2\mu_3)(r_2^2 p_2 - r_3^2 p_3)] \\ u_f|_{r=r_2}^0 = \frac{(1 + \mu_3)r_2}{E_3(r_3^2 - r_2^2)} [r_3^2(p_c - p_3) + (1 - 2\mu_3)(r_2^2 p_c - r_3^2 p_3)] \end{cases}. \quad (9)$$

The displacement of the cement sheath elastic zone is:

$$\begin{cases} u_{ce}|_{r=r_2}^1 = \frac{(1 + \mu_2)r_2}{E_2(r_2^2 - r_p^2)} [r_p^2(p_p - p_2) + (1 - 2\mu_2)(r_p^2 p_p - r_2^2 p_2)] \\ u_{ce}|_{r=r_2}^0 = \frac{(1 + \mu_2)r_2}{E_2(r_2^2 - r_p^2)} [(1 - 2\mu_2)(r_p^2 p_c - r_2^2 p_c)] \\ u_{ce}|_{r=r_p}^1 = \frac{(1 + \mu_2)r_p}{E_2(r_2^2 - r_p^2)} [r_2^2(p_p - p_2) + (1 - 2\mu_2)(r_p^2 p_p - r_2^2 p_2)] \\ u_{ce}|_{r=r_p}^0 = \frac{(1 + \mu_2)r_p}{E_2(r_2^2 - r_p^2)} [(1 - 2\mu_2)(r_p^2 p_c - r_2^2 p_c)] \end{cases}, \quad (10)$$

where $u_{m}|_{r=r_i}^n$ represents the displacement value of the casing-cement sheath-formation system assembly; $m = ca, f$, and ce represent the elastic zone of the casing, formation, and cement sheath, respectively; $n = 0$ represents the stress state of the composite after solidification of the cement stone; $n = 1$ represents the stress state of the composite during fracturing; and r_i represents different radius.

In the plastic zone of the cement sheath, considering the condition of the plane strain model $\varepsilon_z = 0$ and the volume incompressibility, Eq. 11 (Xu and Liu, 1995) can be obtained as follows:

$$\begin{cases} \varepsilon_r + \varepsilon_\theta = 0 \\ \varepsilon_r = \frac{du_{cp}}{dr} \\ \varepsilon_\theta = \frac{u_{cp}}{r} \end{cases}. \quad (11)$$

Using Eq. 11, the aforementioned formula can be written as:

$$\frac{du_{cp}}{dr} + \frac{u_{cp}}{r} = 0. \quad (12)$$

Through the integral formula (Eq. 12), the expression of the cement sheath plastic region u_{cp} is obtained as follows:

$$u_{cp} = \frac{C_1}{r}. \quad (13)$$

TABLE 1 | Physical and mechanical parameters of the casing–cement sheath- formation model.

	Elastic modulus/GPa	Poisson's ratio	Inner diameter/mm	Outer diameter/mm
Casing	200	0.30	129.16	150.24
Cement sheath	10	0.26	150.24	227
Stratum	30	0.20	227	2270

Considering the continuity of the first interface in the casing–cement sheath-formation system, the elastoplastic interface of the cement sheath, and the displacement at the second interface caused by the increase in the internal pressure of the casing, the relationship between the elastic–plastic interface stress of the cement sheath and the first and second interface stresses and by combining the formulas of Eqs 4, 6, 8–10, 13, the system of stress characteristic equations of the system assembly can be obtained.

$$\begin{cases}
 p_p = C \cot \varphi \left[\left(1 + \frac{p_1}{C \cot \varphi} \right) \left(\frac{r_p}{r_1} \right)^{B-1} - 1 \right] \\
 \frac{r_2^2(p_2 - p_p)}{r_2^2 - r_p^2} - \frac{r_p^2 p_p - r_2^2 p_2}{r_2^2 - r_p^2} \sin \varphi + C \cos \varphi = 0 \\
 u_f|_{r=r_2}^1 - u_f|_{r=r_2}^0 = u_{ce}|_{r=r_2}^1 - u_{ce}|_{r=r_2}^0 \\
 u_{ce}|_{r=r_p}^1 - u_{ce}|_{r=r_p}^0 = u_{cp}|_{r=r_p}^1 \\
 u_{ca}|_{r=r_1}^1 - u_{ca}|_{r=r_1}^0 = u_{cp}|_{r=r_1}^1
 \end{cases} \quad (14)$$

Eq. 14 is a five-element equation for the unknown parameters p_1 , p_p , p_2 , r_p , and C_1 . When the casing–cement sheath-formation system assembly is known to receive the internal pressure p_0 , the initial stress p_c , and the formation after cement solidification in the case of far-field stress p_3 , the program is written by MATLAB to solve the stress state, the displacement size, and the elastoplastic interface radius of the cement sheath at the point of the casing pressurization stage.

3 CASE ANALYSIS

3.1 Basic Parameters

According to the current situation of the southwest shale gas well and the possible stress state in the future deep mining process, the physical and mechanical parameters of the casing–cement sheath-stratum combination are selected as shown in Table 1. The maximum site stress p_3 of the stratum is 80 MPa, and the maximum bottom hole pressure in the fracturing construction is 150 MPa. The calculation parameters of the latitude and longitude in Chu and Yang (2015) and Jackson and Murphey (1993) are referenced as follows: the cohesive force of the cement stone is 5.77 MPa, and the internal friction angle is 30°. After the cement is solidified, if the initial stress is affected by the cement type (expansion type and shrinkage type), cement slurry density, and cementing method, etc., then p_c is taken from 0–50 MPa.

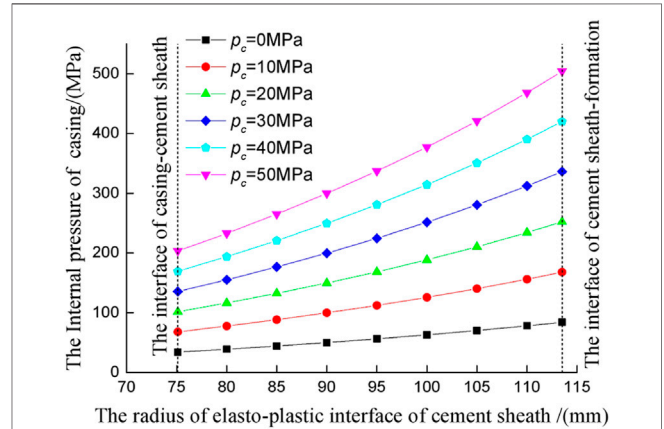


FIGURE 4 | Relationship between the elastoplastic interface and casing pressure.

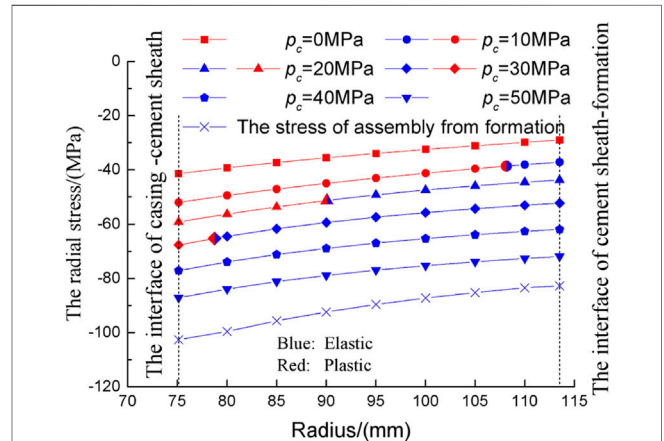


FIGURE 5 | Radial stress distribution of the cement sheath on a casing pressure of 150 MPa.

3.2 Influence of Initial Stress of the Cement Sheath

The relationship between the elastoplastic interface radius and the casing internal pressure under different initial stress conditions of the cement sheath is shown in Figure 4. It can be found from the figure that the smaller the initial stress of the cement sheath, the easier it is to enter the plastic state, and as the internal pressure of the casing increases, the elastoplastic interface gradually expands outward from the first interface, and finally the entire cement sheath enters the plasticity. At the first interface,

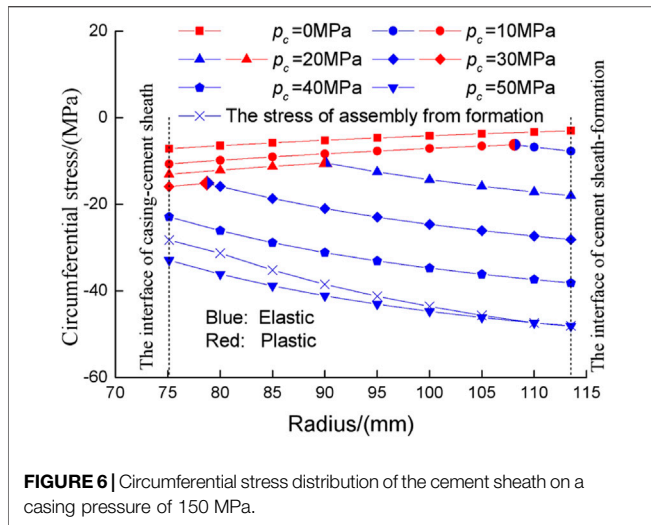


FIGURE 6 | Circumferential stress distribution of the cement sheath on a casing pressure of 150 MPa.

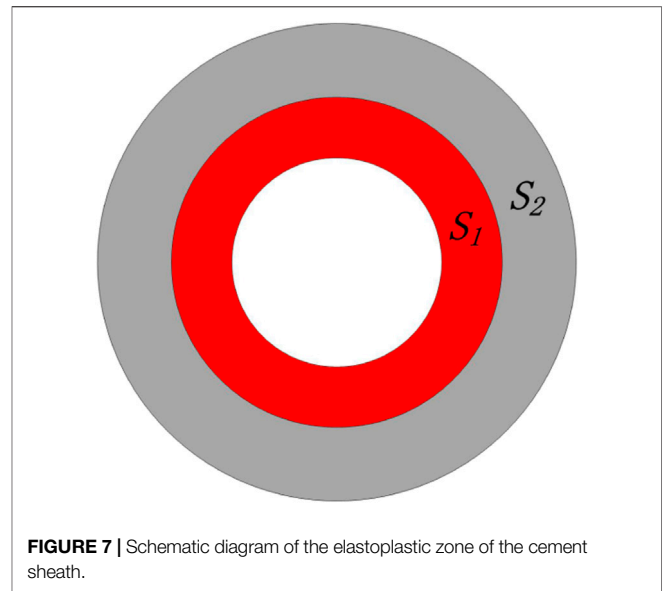


FIGURE 7 | Schematic diagram of the elastoplastic zone of the cement sheath.

the initial stress of the cement sheath is increased from 0 to 50 MPa, and the internal pressure of the casing entering the plastic condition is increased from 33.89 to 203.46 MPa; also, at the second interface, the bottom hole pressure entering the plastic state is higher. When the initial stress of the cement sheath increases from 0 to 50 MPa, the internal pressure of the casing increases from 203.46 to 504.18 MPa.

Figures 5, 6, respectively, show the radial and circumferential stress distribution of the cement sheath when the initial stress of different cement sheaths is 150 MPa inside the casing. When the local stress and the casing internal pressure are directly applied to the combination, the radial compressive stress of the cement sheath is between -102.6 MPa and -82.8 MPa, and the radial stress is greater than the initial stress of the cement sheath from 0 to 50 MPa; the stress is directly applied to the assembly. The circumferential stress is similar to the radial stress at 40–50 MPa. Regardless of whether the cement sheath is in an elastic or plastic state, the radial compressive stress decreases as the radius of the cement sheath increases.

When the initial stress is 0–50 MPa, the initial stress of the cement sheath is larger, and the radial stress is larger; the radial compressive stress is the largest at the first interface and is from -87.16 MPa to -41.37 MPa, and at the second interface, the stress is the smallest one, which is from -71.92 MPa to -29.02 MPa. For the circumferential stress, the variation law is directly related to the elastoplastic characteristics. It shows that as the radius of the cement sheath increases, the circumferential compressive stress of the plastic zone decreases, and the circumferential compressive stress of the elastic zone increases, mainly in three cases: 1) the cement sheath is in a fully plastic state. For example, the initial stress of the cement sheath is 0 MPa, the circumferential stress decreases with the radius of the cement sheath, and the maximum circumferential stress appears at the first interface, which is -7.13 Mpa; the minimum circumferential stress appears at the second interface, which is -3.01 MPa; 2) the inner side of the cement sheath is in a plastic state and the outer side is in an elastic state, i.e., the initial stress of the cement sheath is 10 MPa,

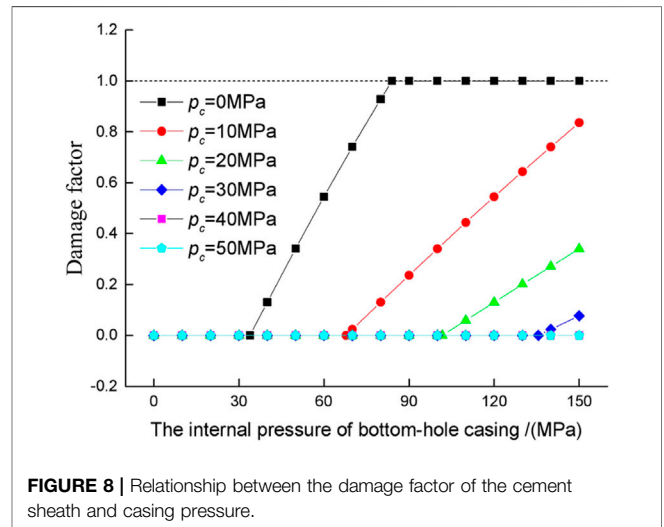


FIGURE 8 | Relationship between the damage factor of the cement sheath and casing pressure.

20 MPa, and 30 MPa, the circumferential compressive stress first decreases and then increases. The circumferential stress is the smallest at the elastoplastic interface, and the maximum circumferential stress is at the first or second interface, depending on the specific situation; (3) the cement sheath is in a fully elastic state, i.e., the initial stress of the cement sheath is 40 and 50 MPa, the circumferential stress increases with the radius of the cement sheath, and the minimum one appears at the first interface, which is from -22.90 MPa to -32.90 MPa; the maximum one appears at the second interface, which is from -38.15 MPa to -48.15 MPa.

3.3 Cement Sheath Damage Analysis

During the fracturing construction process, as the internal pressure of the casing increases, the cement sheath in the elastic state gradually undergoes yield failure from the first interface, entering the plasticity. Then, the plastic volume

gradually increases, and even the entire cement sheath finally enters the plastic state. In this article, the damage factor D is introduced to better describe the damage and failure characteristics of the cement sheath with the increase of the internal pressure of the casing. The damage factor is defined as the ratio of plastic area to total area of the cement sheath. The damage factor $D = 0$ is defined when the cement sheath is all in the elastic state and the damage factor $D = 1$ when the cement sheath is all in the plastic state.

Damage factor:

$$D = \frac{S_1}{S_1 + S_2}, \quad (0 \leq D \leq 1).$$

As shown in **Figure 7**, S_1 represents the area of the plastic zone of the cement sheath section, and S_2 represents the area of the elastic zone of the cement sheath section.

The damage results of the internal pressure of the casing under different initial stress conditions are calculated. As shown in **Figure 8**, the initial stress of the cement sheath has a significant influence on the evolution process of the damage factor during the internal pressure loading process. As the initial stress of the cement sheath increases, the damage appears later or even does not occur, and the rate of damage increases with the increase of internal pressure. When the initial stress is 0 MPa, the cement sheath is damaged when the internal pressure of the casing is 33.89 MPa. When it is only 83.99 MPa, the cement sheath damage factor reaches 1, indicating that the whole enters the plastic state. When the initial stress is 10, 20, and 30 MPa, the corresponding casing internal pressure is 67.81, 101.72, and 135.63 MPa, respectively. When the internal pressure reaching the maximum downhole casing pressure of the oil and gas well is 150 MPa, the damage factors are 0.84, 0.34, and 0.08 and did not enter the plastic state as a whole. When the initial stress is above 40 MPa, even if the internal pressure reaches the maximum casing internal pressure of 150 MPa, the cement sheath can still maintain the damage factor of 0, that is, the cement sheath as a whole is in an elastic state.

4 CONCLUSION

In this article, considering the volume shrinkage, constant, and expansion of the cement slurry during the solidification process, assuming the initial stress state of the cement sheath is 0–50 MPa, a casing–cement sheath–shale formation model is established; the stress state of the cement sheath and the damage characteristics of

the cement sheath during the fracturing process are deduced by the Mohr–Coulomb yield criterion. The conclusions are as follows:

- (1) When the initial stress of the cement sheath is smaller, the radial stress and the circumferential stress are smaller, and the smaller the internal pressure of the casing causing the cement sheath to enter the plastic state, the more likely the damage occurs in the cement sheath.
- (2) The damage factor is introduced. According to the example analysis, the smaller the initial stress of the cement sheath, the earlier the damage occurs, and the damage factor grows faster. When the initial stress of the cement sheath is less than 7.9 MPa, the damage factor D finally reaches 1 with the increase of the internal pressure of the casing; when the initial stress of the cement sheath is greater than 34.2 MPa, although the internal pressure of the casing increases, the damage factor D remains at zero.

DATA AVAILABILITY STATEMENT

The original contributions presented in the study are included in the article/Supplementary Material, further inquiries can be directed to the corresponding authors.

AUTHOR CONTRIBUTIONS

FX: methodology, investigation, and writing–original draft. ZL: data collection and writing–original draft. QR: writing–review and editing. XZ and GY: supervision and validation. HL and HY: data collection. HW seriously participated in the research group Shu Yan, fitted and analyzed the collected data, and prepared for writing the paper.

ACKNOWLEDGMENTS

The authors would like to acknowledge the financial support of the National Key Research and Development Program of China (2018YFC1504903), the Key Projects of Chongqing Science and Technology Bureau (cstc2019jscx-gksbX0071 and cstc2019jscx-gksbX0072), and the Science and Technology Project of Jiangxi Provincial Department of Transportation (2020H0026 and 2020H0052).

REFERENCES

- Chen, Y., Yin, T., and Li, X. (2021). Experimental Investigation on Dynamic Mechanical Behavior and Fracture Evolution of Fissure-Filled Red sandstone after thermal Treatment. *Eng. Geology*. 295, 106433. doi:10.1016/j.enggeo.2021.106433
- Chu, W., and Yang, Y. (2015). Calculation of Micro-annulus Size in Casing–Cement Sheath–Formation System under Continuous Internal Casing Pressure Change. *Pet. Exploration Development* 42 (3), 379–385. doi:10.1016/s1876-3804(15)30033-1
- Deng, J., Wang, K., and Huang, R. (1994). Collapse Resistance of Foil Well Casing–Cement Mantle Combination Subjected to Non-uniform Loading by Rock Creep. *Chin. J. Rock Mech. Eng.* 13 (2), 160–167. doi:10.1007/BF02657007
- Fang, J., Zhao, H., and Yue, B. (1995). Analysis of Loading Property of Casing and Cement Sheath under Nonuniform Geologic Stress. *J. China Univ. Pet.* 19 (6), 52–57.

- Jackson, P. B., and Murphey, C. E. (1993). *Effect of Casing Pressure on Gas Flow through a Sheath of Set Cement*. Amsterdam, Netherlands: SPE 25698-MS. doi:10.2523/25698-MS
- Jin, Y., and Chen, M. (2012). *Borehole Stability Mechanics*. Beijing: Science press.
- Jing, L., Lin, C., and Yang, S. (2009). Theoretical Solution of thermal Stress for Cement Formation Coupling System. *J. China Univ. Pet.* 33 (2), 63–69. doi:10.3321/j.issn:1673-5005.2009.02.012
- Li, J., Chen, M., and Liu, G. (2005a). Elastic-plastic Analysis of Casing-concrete Sheath-Rock Combination. *Acta Petrolei Sinica* 26 (6), 99–103. doi:10.1016/j.molcatb.2005.02.001
- Li, J., Chen, M., and Zhang, H. (2005b). Effects of Cement Sheath Elastic Modulus on Casing External Collapse Load. *J. China Univ. Pet.* 29 (6), 41–44. doi:10.3321/j.issn:1000-5870.2005.06.010
- Li, Y., Liu, S., and Wang, Z. (2010). Analysis of Cement Sheath Coupling Effects of Temperature and Pressure in Non-uniform *In-Situ* Stress Field. *SPE*, 131878. doi:10.2118/131878-ms
- Liu, R., He, Y., Zhao, Y., Jiang, X., and Ren, S. (2020). Tunnel Construction Ventilation Frequency-Control Based on Radial Basis Function Neural Network. *Automation in Construction* 118, 103293. doi:10.1016/j.autcon.2020.103293
- Saint-Marc, J. (2008). “Initial State of Stress: the Key to Achieving Long-Term Cement-Sheath Integrity,” in SPE Annual Technical Conference and Exhibition, Society of Petroleum Engineers. doi:10.2118/116651-ms
- Wang, B., Yan, X., and Yang, X. (2013). Study on Leakage Rate of Natural Gas through an Abandoned Well in Depleted Natural Gas Reservoir Based on SCP. *Sci. Technology Eng.* 13 (26), 7749–7753. doi:10.3969/j.issn.1671-1815.2013.26.028
- Xu, B., and Liu, X. (1995). *Applied Elasticity and Plasticity*. Beijing: Tsinghua University press.
- Xu, F., Tang, S., and Ren, Q. (2021). Experimental Study on the thermal Damage Characteristics of Cement Stone. *Therm. Sci.* 25, 3327–3335. doi:10.2298/tsci200618317x
- Xu, F., Yang, C., and Guo, Y. (2017). Effect of Bedding Planes on Wave Velocity and AE Characteristics of the Longmaxi Shale in China. *Arabian J. Geosciences* 10 (6), 141–150. doi:10.1007/s12517-017-2943-y
- Xu, F., Xu, Z., Tang, S., Ren, Q., Guo, Y., Wang, L., et al. (2022). Evolution of Physical and Mechanical Properties of Cementing Materials during Underground Energy Exploitation and Storage. *J. Energ. Storage* 45, 103775. doi:10.1016/j.est.2021.103775
- Xu, H., Zhang, Z., and Shi, T. (2015). Influence of the WHCP on Cement Sheath Stress and Integrity in HTHP Gas Well. *J. Pet. Sci. Eng.* 126, 174–180. doi:10.1016/j.petrol.2014.11.028
- Yin, Y., Cai, Y., and Chen, Z. (2006). Theoretical Solution of Casing Loading in Non-uniform Ground Stress Field. *Chin. J. Theor. Appl. Mech.* 38 (6), 835–842. doi:10.7623/syxb200604031
- Zhang, J., Zhang, D., and Zhang, Q. (2013). Impact of Elastic Parameters of Cement Ring on Structural Integrity of Casing-Cement Ring-Strata Cementing Combination. *Oil Drilling Prod. Technology* 35 (5), 43–46. doi:10.3969/j.issn.1000-7393.2013.05.012
- Zhang, L., Liu, R., and Zhou, S. (2017). Investigation on Sealing Failure and Improving of Cement Sheath under Simulated Staged Fracturing. *Sci. Technology Eng.* 17 (13). doi:10.3969/j.issn.1671-1815.2017.13.031
- Zhaowei, C., and Yongen, C. (2009). Study on Casing Load in a Casing-Stratum System by Elastoplastic Theory. *Pet. Exploration Development* 36 (2), 119–123. doi:10.3321/j.issn:1000-0747.2009.02.017

Conflict of Interest: Authors FX, ZL, and GY were employed by the company China Merchants Chongqing Communications Research & Design Institute Co., Ltd. Author HY was employed by the company Guangzhou Expressway Co., Ltd.

The remaining authors declare that the research was conducted in the absence of any commercial or financial relationships that could be construed as a potential conflict of interest.

Publisher’s Note: All claims expressed in this article are solely those of the authors and do not necessarily represent those of their affiliated organizations, or those of the publisher, the editors and the reviewers. Any product that may be evaluated in this article, or claim that may be made by its manufacturer, is not guaranteed or endorsed by the publisher.

Copyright © 2022 Xu, Ren, Ling, Yin, Zhou, Liu and Yang. This is an open-access article distributed under the terms of the Creative Commons Attribution License (CC BY). The use, distribution or reproduction in other forums is permitted, provided the original author(s) and the copyright owner(s) are credited and that the original publication in this journal is cited, in accordance with accepted academic practice. No use, distribution or reproduction is permitted which does not comply with these terms.